

Electron cooling forces for highly charged ions in the ESR

T. Winkler*, K. Beckert, F. Bosch, H. Eickhoff, B. Franzke, F. Nolden, H. Reich,
B. Schlitt, M. Steck

GSI, Gesellschaft für Schwerionenforschung mbH, Postfach 110552, D-64220 Darmstadt, Germany

Abstract

In the ESR storage ring fully stripped ions up to uranium have been stored and cooled at beam energies between 50 and 370 MeV/u. Longitudinal cooling forces for heavy ions from C^{6+} to U^{92+} at various energies have been measured with the ESR electron cooler. Two experimental methods have been established which allow the determination of the cooling force for relative ion velocities from zero to 10^7 m/s. At low velocities the equilibrium between cooling and longitudinal heating with rf noise is used. For high relative velocities the cooling force is deduced from the momentum drift of the ion beam after a rapid change of the electron energy. Measurements for several ion species are presented which show a pronounced deviation from the expected q^2 scaling in the regime of the magnetic cooling force. Further investigations have been performed to study the influence of magnetic field strength and beam energy on the longitudinal cooling force.

PACS: 29.20.Dh; 34.50.Bw

Keywords: Electron cooling; ion beam

1. Introduction

Thirty years after Budker's idea [1], electron cooling is now used in many storage rings and has turned out to be an indispensable tool for high precision experiments in atomic and nuclear physics [2,3]. The ESR storage ring at GSI has been used to store and cool heavy ion beams from C^{6+} to U^{92+} in a wide energy range from 50 to 370 MeV/u.

Recombination experiments require a detailed knowledge of effects determining the electron beam temperatures T_{\parallel} and T_{\perp} . Since the electron beam is guided by a longitudinal magnetic field to prevent a radial blow-up due to space charge forces, transverse electric fields cause a cyclotron motion of the electrons. At higher beam energies space charge effects become less important but transverse electric fields in the acceleration gap of the electron beam now determine the transverse motion in the electron beam. An evaluation of the dependence of this electron motion on magnetic field strength and beam energy is important for an improvement of the experimental conditions at the ESR cooler.

The influence of transverse ion velocity components on the cooling force causes the efficiency of electron cooling to drop at high beam energies. A study of this behavior is

necessary for considerations of electron cooling at even higher beam energies.

The electron cooling process described by binary Coulomb collisions between ions and electrons is looked upon in a comoving reference frame, the rest frame of the electron beam. Due to the high beam velocities in the laboratory frame with $\beta = v/c$ between 0.3 and 0.7, relativistic corrections are necessary when transforming into the comoving frame.

2. Electron beam properties

The velocity distribution of the electrons in the comoving frame has a strong influence on the resulting cooling force. It is described by means of the longitudinal and transverse temperature of the electrons:

$$k_B T_{\parallel} = m(\langle v_{\parallel}^2 \rangle - \langle v_{\parallel} \rangle^2), \quad (1)$$

$$k_B T_{\perp} = \frac{m}{2} (\langle v_{\perp}^2 \rangle - \langle v_{\perp} \rangle^2). \quad (2)$$

In the comoving frame $\langle v_{\parallel}^* \rangle$ and $\langle v_{\perp}^* \rangle$ vanish and the electron beam temperatures are given by

$$k_B T_{\parallel}^* = m_e \Delta_{\parallel}^2 \quad \text{and} \quad k_B T_{\perp}^* = \frac{1}{2} m_e \Delta_{\perp}^2 \quad (3)$$

with $\Delta_{\parallel}^2 = \langle v_{\parallel}^{*2} \rangle$ and $\Delta_{\perp}^2 = \langle v_{\perp}^{*2} \rangle$ being the longitudinal and transverse thermal velocities of the electrons. All

* Corresponding author. Tel.: +49 6159 71 2401, fax: +49 6159 71 2985, e-mail: t.winkler@gsi.de.

quantities in the comoving frame are marked with an asterisk.

The velocity distribution of the electrons emitted from a thermionic cathode is isotropic with a temperature of $k_B T \approx 0.11$ eV ($T \approx 1300$ K). The acceleration of the electron beam leads to a reduction of T_{\parallel}^* by several orders of magnitude due to kinematic effects whereas T_{\perp}^* remains unchanged. Now relaxation processes inside the electron beam are responsible for the resulting longitudinal temperature [4]. For the ESR electron cooler we estimate $T_{\parallel}^* = 0.05$ – 0.1 MeV, compared to $T_{\perp}^* = 0.1$ eV. This is described by a “flattened” Maxwellian velocity distribution $f(v_e^*)$ of the electrons in the cooling section

$$f(v_e^*) = \frac{1}{\sqrt{2\pi^3}} \frac{1}{\Delta_{\parallel} \Delta_{\perp}^2} \exp \left\{ -\frac{v_{\parallel}^{*2}}{2\Delta_{\parallel}^2} - \frac{v_{\perp}^{*2}}{\Delta_{\perp}^2} \right\}. \quad (4)$$

In the case of the ESR electron cooler an additional transverse velocity component has to be taken into account. The fast acceleration to energies up to some 100 keV in one gap of about 15 cm length leads to high electric field strengths. Unavoidable transverse components of this accelerating field cause, together with the magnetic field, a transverse cyclotron motion. This additional transverse motion of an electron is dependent on the magnetic field strength and on its distance from the electron beam axis.

Calculations with a computer code [5] evidenced that the particular geometry of the ESR cooler gun yields a contribution to the cyclotron velocity v_c^* that exceeds the thermal component for beam energies above 120 keV for a magnetic field strength of 0.1 T. The calculated velocity of the cyclotron motion as a function of the magnetic field strength for various electron beam energies is displayed in Fig. 1. These calculations assume a radial position of 7.5 mm off the electron beam axis which is the typical

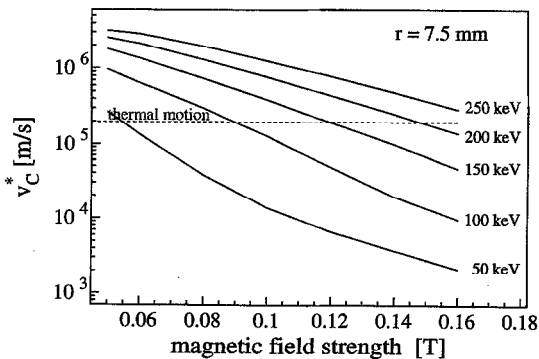


Fig. 1. Calculated velocity of the transverse cyclotron motion 7.5 mm off the electron beam axis as a function of the magnetic field strength at various electron energies. For comparison the thermal component ($kT_{\perp} = 0.1$ eV) of the cyclotron motion is shown.

position of the ion beam due to geometrical constraints in the adjustment of the two beams. As a result of the simulation the cyclotron velocity v_c^* as a function of the accelerating voltage U can be estimated to be

$$v_c^* = 0.26 \text{ m/s} \cdot (U[\text{kV}])^{2.8} \quad (5)$$

for $B = 0.1$ T. To take this additional transverse velocity into account, v_{\perp}^* has to be replaced by $(v_{\perp}^* - v_c^*)$ in Eq. (4) which leads to

$$f(v^*) = N \frac{1}{\sqrt{2\pi^3}} \frac{1}{\Delta_{\parallel} \Delta_{\perp}^2} \exp \left\{ -\frac{v_{\parallel}^{*2}}{2\Delta_{\parallel}^2} - \frac{(v_{\perp}^* - v_c^*)^2}{\Delta_{\perp}^2} \right\}, \quad (6)$$

where N is a numerical normalization factor. Note that v_c^* is constant for all electrons at a given radial position and does therefore not enter into the beam temperature.

3. Cooling force

The description of the cooling force follows a binary collision approach. The friction force is given by energy loss per unit length of an ion of charge qe traveling with velocity v_i^* through an electron gas with velocity distribution $f(v_e^*)$. Neglecting the presence of the magnetic field, the cooling force is given by

$$F_{\parallel}^{nm}(v_i^*) = -F_0 c^2 \int L_C(u) f(v_e^*) \frac{u}{u^3} d^3 v_e^*, \quad (7)$$

where $u = v_i^* - v_e^*$ is the relative velocity between ion and electrons. The factor $F_0 = 4\pi q^2 n_e^* r_e^2 m_e c^2$ contains the dependence of the cooling force on electron density n_e^* and ion charge. r_e denotes the classical electron radius.

The Coulomb logarithm $L_C(u)$ is the result of the integration over the possible impact parameter range $L_C \approx \ln(b_{\max}/b_{\min}) \gg 1$. In most cases it is considered as velocity independent and of the order of 10. The minimum impact parameter b_{\min} is set to $b_{\perp} = (qr_e c^2)/u^2$, the impact parameter for 90° scattering, whereas b_{\max} is determined by the presence of the magnetic field. As long as the interaction time $\tau = b_{\max}/u$ is short compared to the inverse cyclotron frequency ω_c , the influence of the magnetic field is neglected and the free electron gas approximation holds. Therefore $b_{\max} = 2\pi u/\omega_c$ is chosen for the non-magnetic case. However, the above approximation for L_C is not valid for heavy ions with high charge states and low velocities because it yields negative values. To avoid this

$$L_C(u) = \frac{1}{2} \ln \left(1 + \frac{b_{\text{mag}}^2}{b_{\min}^2} \right) \quad (8)$$

is used [6]. This more accurate expression for the Coulomb logarithm is not limited to $L_C \gg 1$.

Impact parameters larger than b_{mag} lead to interaction

times much longer than the cyclotron period. The ion now sees a point-like charge moving along the center of the helical electron orbit with only a longitudinal degree of freedom. Accordingly the transverse velocity distribution of the electrons does not enter into the kinematics of this kind of interaction with magnetized electrons. One has to replace \mathbf{u} by $\mathbf{u}^{\text{ad}} = \mathbf{v}_i^* - \mathbf{v}_{e\parallel}^*$ and L_c by $L_c^{\text{ad}} = \ln(b_{\text{max}}/b_{\text{mag}})$ with b_{max} equal to the radius of the electron beam. Following the discussion in Ref. [7], the magnetic part of the electron cooling force is

$$F_{\parallel}^{\text{ad}}(v_i^*) = -\frac{F_0 c^2}{2} \int L_c^{\text{ad}}(u^{\text{ad}}) f(v_e^*) 3 \frac{u_{\perp}^{\text{ad}2} u_{\parallel}^{\text{ad}}}{u^{\text{ad}5}} d^3 v_e^*. \quad (9)$$

This contribution of the cooling force is very sensitive to $u_{\perp}^{\text{ad}} = v_{i\perp}^*$, the transverse component of the ion motion in the electron rest frame. Such transverse components are caused, e.g., by the ion beam divergence in the cooler section and alignment errors of the two beams or magnetic field inhomogeneities, and are strongly dependent on the beam energy. An average angle θ between the ion trajectory and the electron beam axis will lead to a transverse velocity in the comoving frame of $u_{\perp}^{\text{ad}} = \gamma \beta c \theta$. This will reduce the efficiency of magnetic cooling for higher beam energies for a given θ .

4. Measurement of the longitudinal cooling force

To study the behavior of the cooling force in detail, precision measurements of absolute cooling forces as a function of the ion velocity are necessary. At the ESR two methods are used which cover the whole ion velocity range from zero to some 10^7 m/s.

The principle of the first method was originally developed at LEAR [8] and was further improved and calibrated at the ESR. Here the equilibrium between a longitudinal heating of the ion beam and electron cooling is used. The heating is performed by applying a suitable random noise signal at a certain harmonic of the revolution frequency of the ion beam. This heating causes a diffusion of the ions in longitudinal velocity space which is counteracted by the cooling force. In equilibrium the cooling force is proportional to the diffusion constant $D_{v_{\parallel}}^*$ of the applied heating times the logarithmic derivative of the ion beams velocity distribution $\psi(v_{\parallel}^*)$:

$$F_{\parallel}^*(v_{\parallel}^*) \propto D_{v_{\parallel}}^* \frac{\partial \psi(v_{\parallel}^*) / \partial v_{\parallel}^*}{\psi(v_{\parallel}^*)} \quad (10)$$

This heating method is applicable for ion velocities from zero to some 10^4 m/s.

The second method covers high ion velocities between 10^4 and 10^7 m/s. The drag force exerted on the ion beam as a whole is measured using the drift velocity of the ion

beam in momentum space after changing the electron beam energy:

$$F_{\parallel}^* = \frac{\Delta p^*}{\Delta t^*}. \quad (11)$$

The acceleration voltage of the electron beam is changed by a sudden variable step between 10 and 5000 V and after a time delay the momentum distribution of the ion beam is measured with a fast Schottky scan. Both methods are described in more detail elsewhere [9,10].

5. Cooling forces for different ion species

Longitudinal cooling forces could be measured at the ESR for a number of ion species from C^{6+} to U^{92+} . To allow a comparison of the different measurements they were performed under as equal conditions as possible concerning alignment of electron and ion beam, magnetic field strength, ion beam position and energy. All absolute cooling forces are normalized to an electron density of $1 \times 10^6 \text{ cm}^{-3}$. Some measurements for different ion species are shown in Fig. 2. The continuous curves at low ion velocities are results of the heating method whereas the data points are obtained by the voltage step technique. Both methods are calibrated independently and show an excellent agreement of the absolute values for the cooling force within the accuracy of 20%.

All measured longitudinal cooling forces reach their maximum value at ion velocities of about 2×10^4 m/s. They show a linear increase of the friction force at low ion

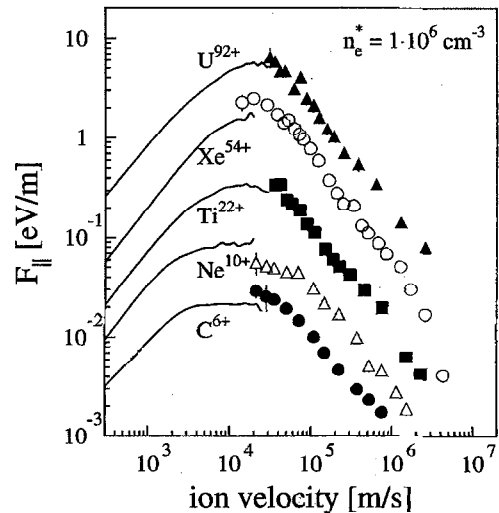


Fig. 2. Measured longitudinal cooling force for various ion species normalized to an electron density of $1 \times 10^6 \text{ cm}^{-3}$. The continuous curves at low ion velocities are results of the heating method whereas the data points are obtained by the voltage step technique. Both methods are calibrated independently.

velocities and a $1/v_i^{*2}$ dependence in the high velocity regime.

6. Charge dependence of the cooling force

The description of the cooling force on the basis of binary Coulomb collisions results in a q^2 scaling of the cooling force with the ion charge, neglecting a weak charge dependence of the Coulomb logarithm. The large number of measured cooling forces for different ion species with $6 \leq q \leq 92$ obtained at the ESR allowed us to extract the charge scaling even for highly charged ions. During this investigation it turned out that the charge scaling is dependent on the ion velocity.

The power x of the charge scaling was determined by fitting a q^x dependence to measured cooling forces at a certain ion velocity. The resulting power as a function of the ion velocity is shown in Fig. 3. A distinct variation of x between 1.7 and 2.1 was found. According to the theoretical description of the cooling force the resulting force is dominated by $F_{\parallel}^{\text{ad}}$ for ion velocities below some 10^5 m/s. At higher ion velocities $F_{\parallel}^{\text{nm}}$ determines the cooling force. So the observed variation of the charge scaling is mainly related to the magnetic cooling force. The again increasing power in the high ion velocity regime is due to the increasing influence of the non-magnetic cooling force. This observed charge scaling is not reproduced by the theoretical description which yields a q^2 scaling for $F_{\parallel}^{\text{ad}}$.

7. Energy dependence

The cooling process in the comoving reference frame is, apart from relativistic transformation effects, independent of the beam energy. Measurements of cooling forces at different beam energies between 50 and 370 MeV/u revealed an increase of the cooling force by more than one

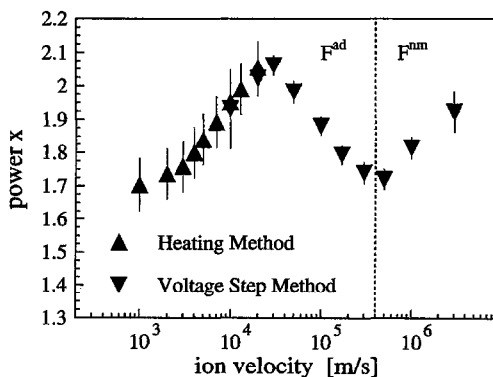


Fig. 3. Variation of the power of the charge scaling of the longitudinal cooling force with the ion velocity.

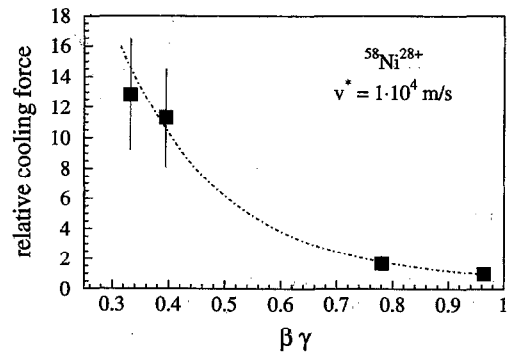


Fig. 4. Relative change of the longitudinal cooling force for Ni^{28+} at an ion velocity of 10^4 m/s as a function of $\beta\gamma$, with the value at 370 MeV/u as reference. The dash-dotted curve shows the calculated relative change of $F_{\parallel}^{\text{ad}}$ due to the dependence of u_{\perp}^{ad} on $\beta\gamma$.

order of magnitude towards lower beam energies. The observed relative increase of the cooling force at an ion velocity of 10^4 m/s for a Ni^{28+} beam as a function of $\beta\gamma$ is displayed in Fig. 4.

The increase of the cooling force by a factor of 13 when reducing the ion beam energy from 370 to 50 MeV/u can be explained by the influence of the transverse ion velocity u_{\perp}^{ad} on the magnetic cooling force. The calculated relative increase of $F_{\parallel}^{\text{ad}}$ according to the dependence of u_{\perp}^{ad} on $\beta\gamma$ is shown as a dash-dotted curve in Fig. 4, assuming an average angle $\theta = 0.2$ mrad.

8. Influence of the magnetic field strength

An investigation of the magnetic field strength dependence of the electron cooling force will be a test for the validity of the binary collision model and the separation of the cooling force into a magnetic and non-magnetic contribution. Measurements of cooling forces at different magnetic field strengths of 0.11 and 0.15 T revealed no significant influence.

On the other hand we know that the transverse motion of the electrons is strongly dependent on the magnetic field (Fig. 1). A sensitive tool to investigate this dependence is the radiative recombination (RR) of ions with electrons in the cooler [11]. The rate coefficient was found to increase with the magnetic field strength, a behavior that could be explained using the calculated dependence of v_{\perp}^* on B . In that way the RR was used as a diagnostic tool for the transverse electron velocity distribution, a property to which the electron cooling force is not sensitive.

Furthermore these experiments proved the presence of magnetic electron cooling. The fact that the cooling force, measured in an ion velocity regime where the magnetic cooling force is supposed to dominate, is independent of the magnetic field strength and therefore from the trans-

verse electron motion strongly supports the described model. This is another proof for the existence of magnetic electron cooling besides the observed values for the cooling force for adiabatically expanded electron beams [12].

References

- [1] G.I. Budker, Sov. J. Atom. Energy 22 (1967) 438.
- [2] H. Poth, Phys. Rep. 196 (1990) 135.
- [3] I.N. Meshkov, Phys. Part. Nucl. 25 (1994) 631.
- [4] V.I. Kudelainen, V.A. Lebedev, I.N. Meshkov, V.V. Parkhomchuk and B.N. Sukhina, Sov. Phys. JETP 56 (1982) 1191.
- [5] W.B. Hermannsfeldt, SLAC-226 (1979).
- [6] G.H. Jansen, Coulomb Interactions in Particle Beams (Academic Press, San Diego, 1990) chap. 4.
- [7] Ya.S. Derbenev and A.N. Skrinsky, Part. Acc. 8 (1978) 235.
- [8] H. Poth, W. Schwab, B. Seligmann, M. Wörtge, S. Baird, J. Bosser, M. Chanel, H. Haseroth, C.E. Hill, R. Ley, D. Manglunki, D. Möhl, G. Tranquille and J.L. Vallet, Nucl. Instr. and Meth. A 287 (1990) 328.
- [9] T. Winkler, K. Beckert, F. Bosch, H. Eickhoff, B. Franzke, O. Klepper, F. Nolden, H. Reich, B. Schlott, P. Spädtke and M. Steck, Hyperfine Int. 99 (1996) 277.
- [10] T. Winkler et al., to be published.
- [11] H.F. Beyer, D. Liesen and O. Guzman, Part. Acc. 24 (1989) 163.
- [12] S. Pastuszka, U. Schramm, M. Grieser, C. Broude, R. Grimm, D. Habs, J. Kenntner, H.-J. Miesner, T. Schüsler, D. Schwalm and A. Wolf, Nucl. Instr. and Meth. A 369 (1996) 11.